Journal of Crystal Growth 394 (2014) 89–96

Contents lists available at ScienceDirect

Journal of Crystal Growth

journal homepage: www.elsevier.com/locate/jcrysgro

Effect of sample size on intermetallic Al_2Cu microstructure and orientation evolution during directional solidification

Ka Gao [a], Shuangming Li [a,*], Lei Xu [b], Hengzhi Fu [a]

[a] State Key Laboratory of Solidification Processing, Northwestern Polytechnical University, Xi'an 710072, China
[b] College of Materials Science and Engineering, Qingdao University of Science and Technology, Qingdao 266042, China

ARTICLE INFO

Article history:
Received 7 December 2013
Received in revised form
28 January 2014
Accepted 7 February 2014
Communicated by M. Rettenmayr
Available online 22 February 2014

Keywords:
A1. Characterization
A1. Crystal morphology
A1. Dendrites
A1. Directional solidification
A2. Double crucible technique
B1. Alloys

ABSTRACT

Al–40% Cu hypereutectic alloy samples were successfully directionally solidified at a growth rate of 10 μm/s in different sizes (4 mm, 1.8 mm, and 0.45 mm thickness in transverse section). Using the serial sectioning technique, the three-dimensional (3D) microstructures of the primary intermetallic Al_2Cu phase of the alloy can be observed with various growth patterns, L-shape, E-shape, and regular rectangular shape with respect to growth orientations of the (110) and (310) plane. The L-shape and regular rectangular shape of Al_2Cu phase are bounded by {110} facets. When the sample size was reduced from 4 mm to 0.45 mm, the solidified microstructures changed from multi-layer dendrites to single-layer dendrite along the growth direction, and then the orientation texture was at the plane (310). The growth mechanism for the regular faceted intermetallic Al_2Cu at different sample sizes was interpreted by the oriented attachment mechanism (OA). The experimental results showed that the directionally solidified Al–40% Cu alloy sample in a much smaller size can achieve a well-aligned morphology with a specific growth texture.

1. Introduction

Dendrite is a fundamental growth pattern in alloy solidification. Normally, dendrites form in a specific growth orientation termed as "preferred growth direction" whether the alloy is in free growth or directional solidification. The effect factors on the preferred growth direction have attracted considerable interests [1–7]. For instance, Haxhimali et al. [6] showed that the preferred growth direction and microstructure of Al dendrites in directionally solidified Al–Zn alloys depend on the composition of the alloy. Amoorezaei et al. [8] pointed out that the dendrite orientation selection is influenced not only by the alloy composition, but also by the solidification parameters, such as thermal gradient and pulling velocity in directional solidification. It should be noted that these investigations mainly focus on the growth of simple Al dendrites solid solution. For complex intermetallics in solidification, not much light has been shed on the microstructures relative to certain preferred growth directions.

Intermetallic Al_2Cu phase has crystalline anisotropy; thus it displays various growth patterns and specific growth direction in different conditions. C.J. Li et al. [9] investigated the growth behavior of Al_2Cu phase of directionally solidified Al–25 at% Cu hypereutectic alloy, and they observed that primary Al_2Cu phases oriented along a magnetic field and grew into various patterns structured at different cooling rates. R. Hamar et al. [10] studied the effect of alloy composition on the orientation of Al_2Cu phase dendrite and they found that with increase in alloy composition the phase orientation changed from the plane {110} to {112} or {202}. Yilmaz and Elliott [11] found that Al_2Cu phase of Al–40% Cu alloy showed different growth modes and structures at different directionally solidified rates. These experimental results demonstrate that the microstructure and orientation of Al_2Cu phase are related with the alloy composition and the growth rate in directional solidification.

However, Trivedi et al. [12] found thermosolutal convection in directional solidification. The strength of melt convection can be characterized by a Rayleigh number (Ra), and the magnitude of the Rayleigh number is proportional to the sample diameter. To discuss and eliminate the effect of convection on the solidified microstructures and orientations, they proposed a method to be used in a capillary sample to acquire a pure diffusion solidification condition and found that in directionally solidified Al–4% Cu alloy the Al dendrites could grow in pure diffusion regime when the sample diameter was less than 1 mm (0.8 mm). It indicates that the sample size can affect the solidified microstructure and orientation. There is a need to study the effect of sample size on

* Corresponding author. Tel.: +86 29 88493264.
E-mail address: lsm@nwpu.edu.cn (S. Li).

http://dx.doi.org/10.1016/j.jcrysgro.2014.02.023
0022-0248

the microstructure and orientation. In addition, in directionally solidified Al–40% Cu alloy, the convection was still present and faceted L-shape Al_2Cu dendrites developed in the solidified microstructures. The Al_2Cu dendrites corresponding to the preferred growth direction have not been investigated.

In this study, we present a novel method in which micro-thermosolutal convention solidification can be achieved by reducing the sample size. Using the serial sectioning technique, the three-dimensional (3D) microstructures and crystal orientation of intermetallic dendrites Al_2Cu were investigated by changing the sample size. This experimental method is easy to conduct and different from the conventional way to change alloy composition or solidification parameters, such as thermal gradient and growth rate. The experimental results show that the small directionally solidified samples can obtain a regular microstructure with a specific growth direction of the intermetallic Al_2Cu alloy.

2. Experimental procedures

2.1. Materials

Al–40 wt% Cu hypereutectic alloy was prepared in a vacuum induction melting furnace with purity aluminum (99.8 wt%) and copper (99.5 wt%). The composition of the ingot measured by chemical titration was Al–39.2 wt% Cu. The experimental sample sizes were 4 mm, 1.8 mm, and 0.45 mm (thickness). Fig. 1 presents the schematic drawing of the samples with different sizes. In Fig. 1a, the 4 mm sample was put inside a high-purity alumina crucible. They were assembled together with the sample length of 100 mm as shown in Fig. 1b. In order to reduce melt convection in the Al–Cu hypereutectic alloy, a device was designed as shown in Fig. 1c and d, and the directionally solidified sample was embedded in the middle of two crucibles (inner crucible with a diameter of 3.1 mm and outer crucible of 4 mm). In this case, the thickness of the sample is only 0.45 mm, which is greatly reduced compared with 0.8 mm and this sample in our method is different from the capillary sample introduced by Trivedi et al. [12]. Consequently, the melt may solidify in the micro-convection condition because melt convection intensity is proportional to the size of the sample. Moreover, the thickness of the sample can be further reduced by increasing the size of the inner crucible. Then, the two crucibles were mounted onto the withdrawing bar.

2.2. Sample preparation

Directional solidification experiments were carried out using a Bridgman vertical vacuum furnace described elsewhere [13]. The thermal gradient was measured using a Φ0.5 mm NiCr–NiSi thermocouple, which was embedded in a sample put inside the crucible of 4 mm and the inner crucible with a diameter of 3.1 mm. The sample was preheated by a graphite heater at 700 °C for 20 min to homogenize the original sample composition. Then the NiCr–NiSi thermocouple and the sample were moved downwards synchronously at a pulling velocity of 10 μm/s. At the same time, the temperature curve was measured by thermometric instruments, and the thermal gradient was calculated and its average value was about 250 K/cm.

In the directional solidification process, when the directional solidification distance reached 50 mm, the sample was quenched into a liquid Ga–In–Sn pool to keep the S/L interface. In addition, the growth rate is substituted for the pulling velocity in this paper,

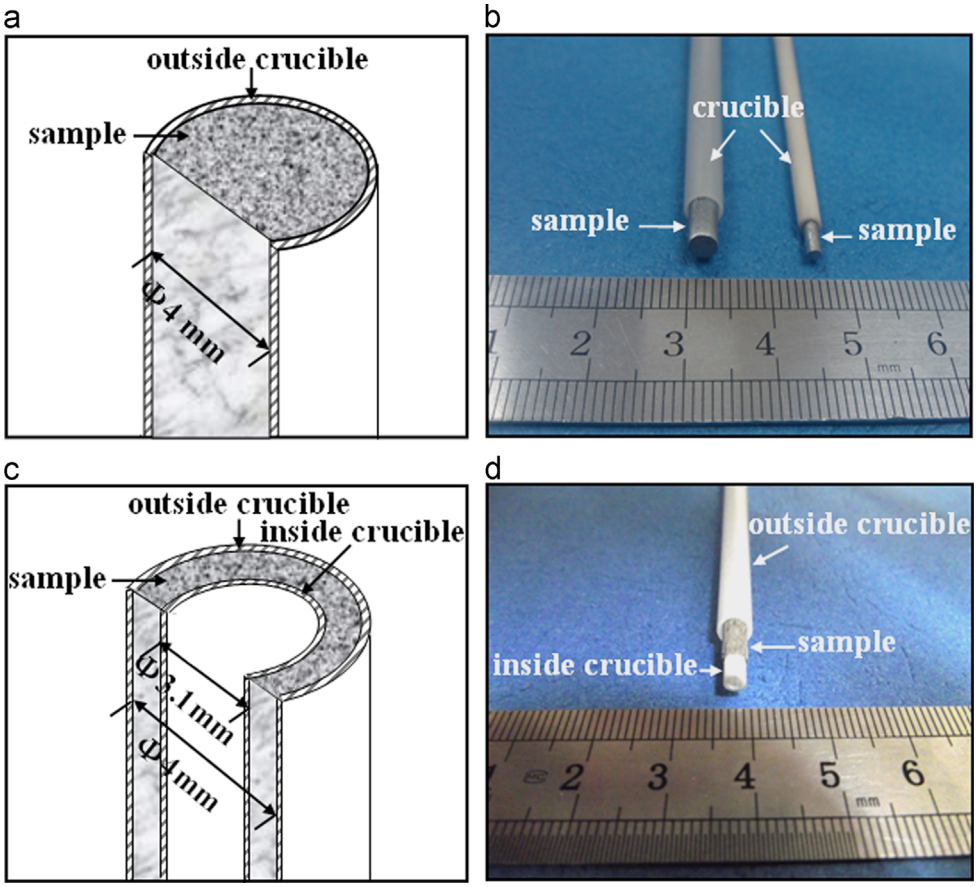

Fig. 1. (a) The schematic drawing of the 4 mm sample under directional solidification, (b) 4 and 1.8 mm experimental samples, (c) the schematic drawing of the 0.45 mm sample under directional solidification, and (d) the 0.45 mm experimental sample.

because it is the same as the solidification process achieves the steady state after a short initial transient zone during directional solidification.

2.3. Characterization

The directionally solidified samples were sectioned horizontally and vertically to the growth direction. The microstructures of the polished samples were revealed with the agent of H_2O (46 mL)+HNO_3 (3 mL)+HF (1 mL) for about 15 s. A Lecia DM4000M optical microscope and a scanning electron microscope (SEM, JSM-6390A) were employed to photograph the microstructures of the samples. The Mimics (Materialise's interactive medical image control system) software was applied to reconstruct the three-dimensional (3D) microstructures images of the primary Al_2Cu phase. X-ray powder diffraction (XRD, D/max-3) was used to determine the orientation. In addition, a transmission electron microscope (TEM, Tecnai G^2 F30) was employed to observe the faceted plane.

3. Results

3.1. Directionally solidified microstructures (2D and 3D)

The microstructures in the longitudinal section of directionally solidified Al–40% Cu alloy samples in different sizes are shown in Fig. 2. It is well-known that the solidified microstructures of Al–40% Cu alloy consist of primary intermetallic θ-Al_2Cu and eutectic (Al/Al_2Cu) based on the Al–Cu phase diagram. The primary Al_2Cu phase can be clearly distinguished from the eutectic (Al/Al_2Cu) in the solidified alloy, since the size of the primary phase is one magnitude order larger than that of the eutectic. As seen in Fig. 2a, the primary Al_2Cu phase is the faceted L-shaped phase [13] and the refined eutectic structure is in between.

Unlike the microstructure pattern in Fig. 2a, the primary phase in the 1.8 mm sample assumed an elongated plate-like morphology in Fig. 2b. The growth direction of the phase did not align parallely to the heat flux direction. When the sample size was reduced to 0.45 mm, the primary intermetallic Al_2Cu developed a parallelogram pattern as shown in Fig. 2c. Different from those in the 4 mm and 1.8 mm samples, there was only a single layer of Al_2Cu dendrite in the microstructure and the dendrite growth direction was along the pulling direction. Through measurement and calculation, the thermal gradient in the 4 mm sample was found to be about 236 K/cm, which is less than that in the 0.45 mm sample with 255 K/cm. It indicates that when the sample is smaller, its thermal gradient will be higher. However, the minimal changes in the temperature gradient in different size samples could not result in more effects on morphology evolution. It can deduce that the effect of the temperature gradient change on microstructures during directional solidification is small.

Fig. 3 shows the transverse-section microstructures of samples directionally solidified in different sizes. In the 4 mm sample, the primary phase developed a faceted L-shaped pattern as shown in Fig. 3a. With a reduction in sample size, the faceted L-shaped Al_2Cu shrunk and gradually merged into an E-shaped morphology as indicated in Fig. 3b.

When the sample size was reduced further to 0.45 mm, the primary phase of the sample formed a well-aligned pattern, as shown in Fig. 3c, where a single layer of the Al_2Cu dendrite was observed at the right side of Fig. 3c and multilayer of the dendrite at the left side. The space limitation seems to change nothing in the morphology of the Al_2Cu dendrite as the primary Al_2Cu dendrite grew into a rectangular shape and the eutectic (Al/Al_2Cu) appeared in the center. Those patterns were magnified in Fig. 3c, different from the microstructures observed in Fig. 3a and b. The formation mechanism of these different shapes of the primary intermetallic Al_2Cu is discussed later in this paper.

In addition, using the serial sectioning technique [14,15], the three-dimensional (3D) microstructures of the primary Al_2Cu

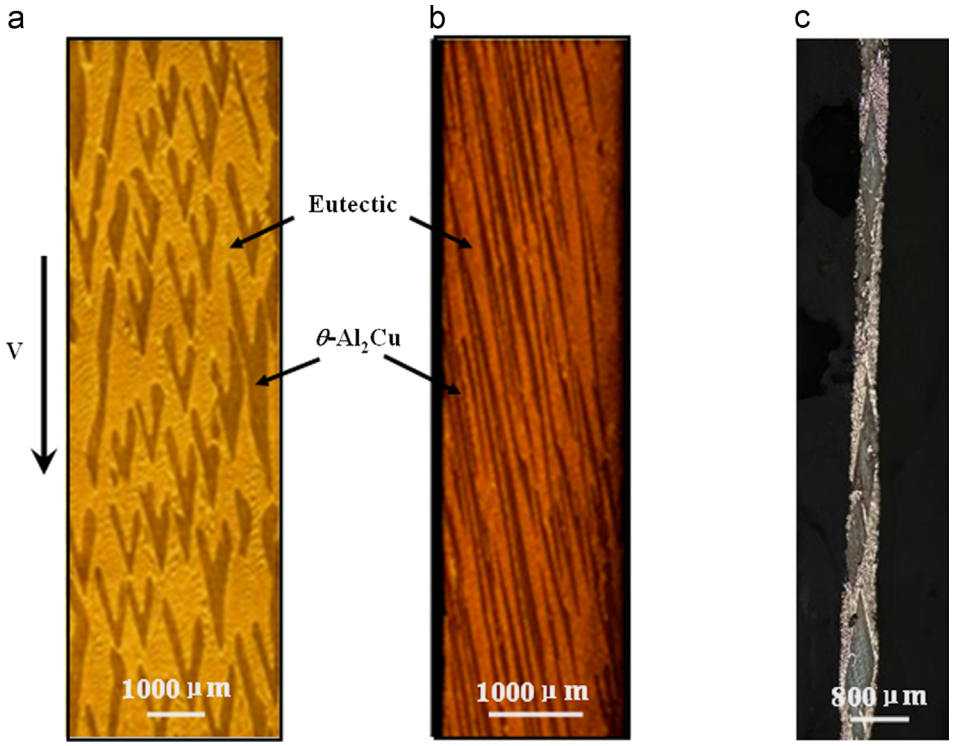

Fig. 2. Directional solidification microstructures of Al–40% Cu hypereutectic alloy in the longitudinal section at a solidification rate of V=10 μm/s: (a) 4 mm sample, (b) 1.8 mm sample, and (c) 0.45 mm sample.

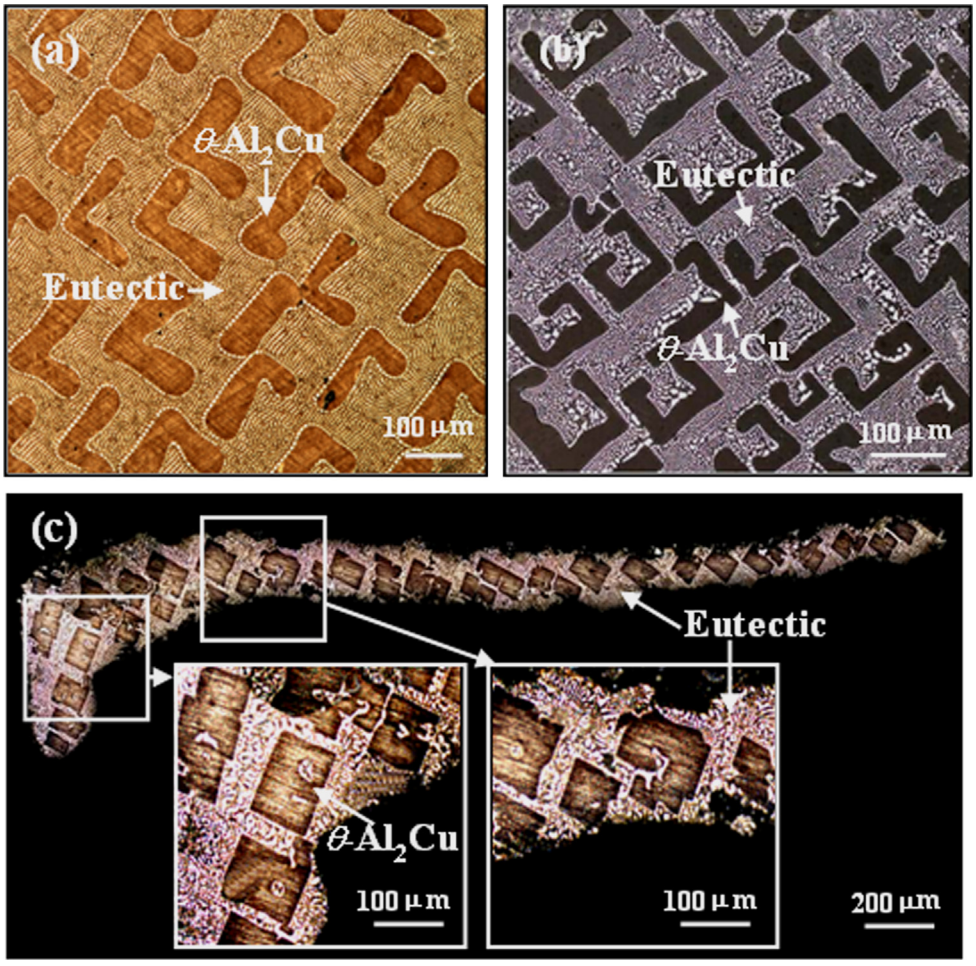

Fig. 3. Directionally solidified microstructures of Al–40% Cu hypereutectic alloy in the transverse section: (a) 4 mm sample, (b) 1.8 mm sample and (c) 0.45 mm sample.

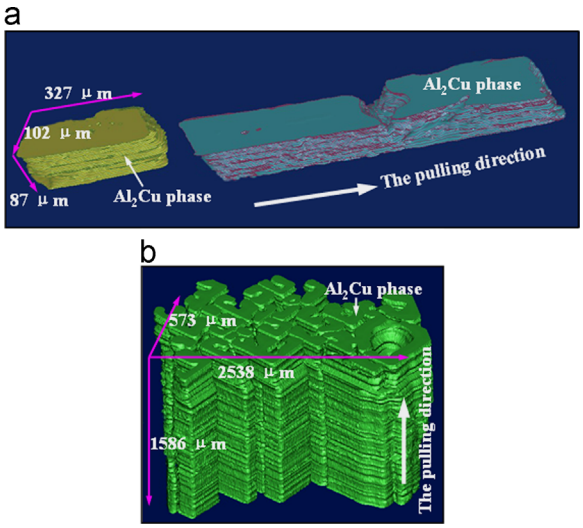

Fig. 4. The 3D microstructure of the primary Al_2Cu phases during directional solidification of the Al–40% Cu alloy: (a) 0.45 mm sample and (b) 4 mm sample.

phase of Al–40% Cu hypereutectic alloy were reconstructed in different size samples during directional solidification shown in Fig. 4. Three-dimensional (3D) microstructures can clearly reveal the size, shape and distribution of the phases, providing a novel way to deeply understand the formation mechanism of the solidified phases. In our study, the results show that in the 0.45 mm sample, the primary Al_2Cu phase was observed rectangularly parallelepiped and grew along the solidification direction as shown in Fig. 4a. It is not difficult to know that the 2D morphologies of the Al_2Cu phase in the transverse section displayed the rectangular shape, which is consistent with the result in Fig. 3c. Similar to the result in the 0.45 mm sample, the 2D morphologies of the Al_2Cu phase in the transverse section of the 4 mm sample displayed an I-shaped pattern and grew along the solidification direction, as shown in Fig. 4b, which is consistent with the result shown in Fig. 3a. The 2D morphologies given were broadly representative and typical for factual morphologies of the Al_2Cu phase and have already displayed the true information of the 3D microstructures. It can be deduced that the growth mechanism as deduced from the 2D microstructures is convincing.

3.2. XRD orientation analysis

For clarifying the crystallographic characterization of the Al_2Cu phase, XRD was used to measure the growth orientation of the primary phase. The measured result is shown in Fig. 5. Various characteristic peaks of the Al_2Cu phase in the as-cast ingot sample, e.g., (110), (310), (200), (211), (112), (202), and (420), could be determined accurately. The diffraction intensity of (110) is the highest, indicating that the (110) plane is the preferred growth plane of the phase, the same as reported by the literature [16]. Whereas in the directionally solidified 4 mm and 1.8 mm samples, only two peaks of the phase, (110) and (310), were evident in Fig. 5. The diffraction intensity of (310) solidified in the 1.8 mm sample was slightly larger than that of the plane (110). That is, a noticeable texture orientation at (310) was formed.

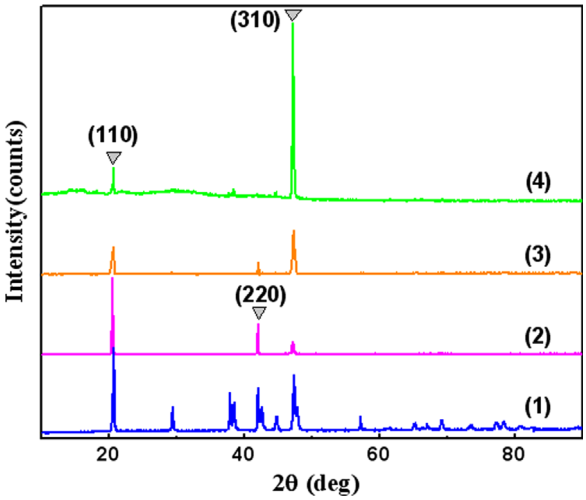

Fig. 5. XRD patterns for directionally solidified Al–40 wt% Cu alloy at a solidification rate of $V=10$ μm/s: (1) free solidification, (2) 4 mm sample, (3) 1.8 mm sample, and (4) 0.45 mm sample.

When the sample size was further reduced to 0.45 mm, the (310) plane corresponded to the strongest diffraction intensity of the phase. It seems that the preferred growth plane of the phase turned from the (110) plane to the (310) one. The experimental results are different from the reported experiments [17,18] in that the Al_2Cu phase was directionally solidified with a preferred growth direction (110) by applying a high magnetic field at an age-hardened state.

Because of the convection effects, the preferred growth plane of Al_2Cu changes from (110) to (310) with the sample size decreasing from 4 mm to 0.45 mm. Trivedi et al. [19] found that if the sample diameter is less than about 1 mm, then the convective transport will become very weak by reducing the sample diameter and molecular diffusion will be the dominant mode of solute transport. When the sample size decreased from 4 mm to 0.45 mm, the microstructures formed under diffusive growth conditions. The solute diffusion would be influenced to slow down and its equivalent boundary layer would be decreased [20]. Then the rate of atoms deposition on different crystal planes would be changed, which is related on the face attachment energy. Atoms aggregated easily on the crystal plane with higher attachment energy, because of the fewer satisfied bonds. The attachment energy of the crystal plane (310) is higher than that of the crystal plane (110) [10], which has fewer satisfied bonds. Subsequently, atoms could easily transfer and build up on this plane. Then the (310) direction would become predominant. The phase will grow more rapidly along the normal direction of the (310) crystal plane than in the (110) direction.

3.3. *Bounded surfaces of Al_2Cu phase observed by TEM*

To explain the growth mechanism of the primary Al_2Cu phase in the directionally solidified Al–40% Cu alloy, the bounded surfaces of the phase were determined. Due to the Gibbs–Curie–Wulf law [21] states, the preferred growth direction will be along the crystal plane direction with the highest attachment energy. Hamar and Lemaignan [10] gave the attachment energies for the main surface planes of the Al_2Cu phase. Assuming the growth rates to be proportional to the attachment energy of each plane, a theoretical habit of the Al_2Cu crystal can be obtained by crystal growth simulation. The resultant growth morphology is shown in Fig. 6. It shows a tendency toward columnar growth along the [001] axis. The phase morphology was faceted rectangular pattern in the transverse section, and the four rectangular edges were {110} facets. It demonstrated that the Al_2Cu phase was bounded by {110} facets.

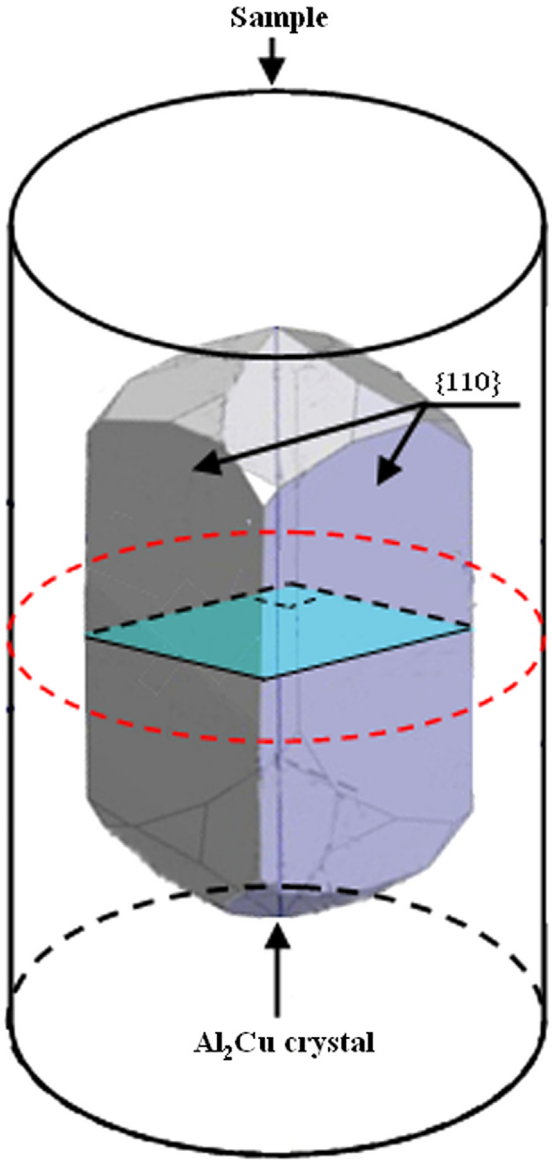

Fig. 6. Growth morphology of the Al_2Cu crystal.

In order to verify the above simulation results, we employed TEM to investigate the facets of Al_2Cu phase in different size samples. Al_2Cu phase in the 0.45 mm sample was in a rectangular pattern in the transverse section and bounded by faceted planes shown in Fig. 7a. Fig. 7b shows a TEM image of the microstructure of the red region. The black area structure can be identified as the Al_2Cu phase. Fig. 7c shows a selected-area electron diffraction pattern (SAED) from the Al_2Cu phase shown in Fig. 7b. The [001] zone axis was chosen to be parallel to the electron beam. By indexing the diffraction patterns, the {110} facets of Al_2Cu phase shown in Fig. 7c can be clearly identified. Moreover, these diffraction patterns can show the faceting characteristic as the rectangular pattern in Fig. 7a. The bounded surfaces of regular rectangular pattern of Al_2Cu phase are the {110} facets shown in Fig. 7d, which correspond to the simulation results shown in Fig. 6.

Meanwhile, the L-shaped morphology in the 4 mm sample is observed in Fig. 8a. The L-shaped morphology of the Al_2Cu phase was also bounded by faceted planes. Fig. 8b shows a TEM image of the microstructure of the red region and Fig. 8c shows a selected-area electron diffraction pattern from the Al_2Cu phase in Fig. 8b. By indexing the diffraction patterns, the four diffraction patterns shown in Fig. 8c can be identified to be the {110} facets of the

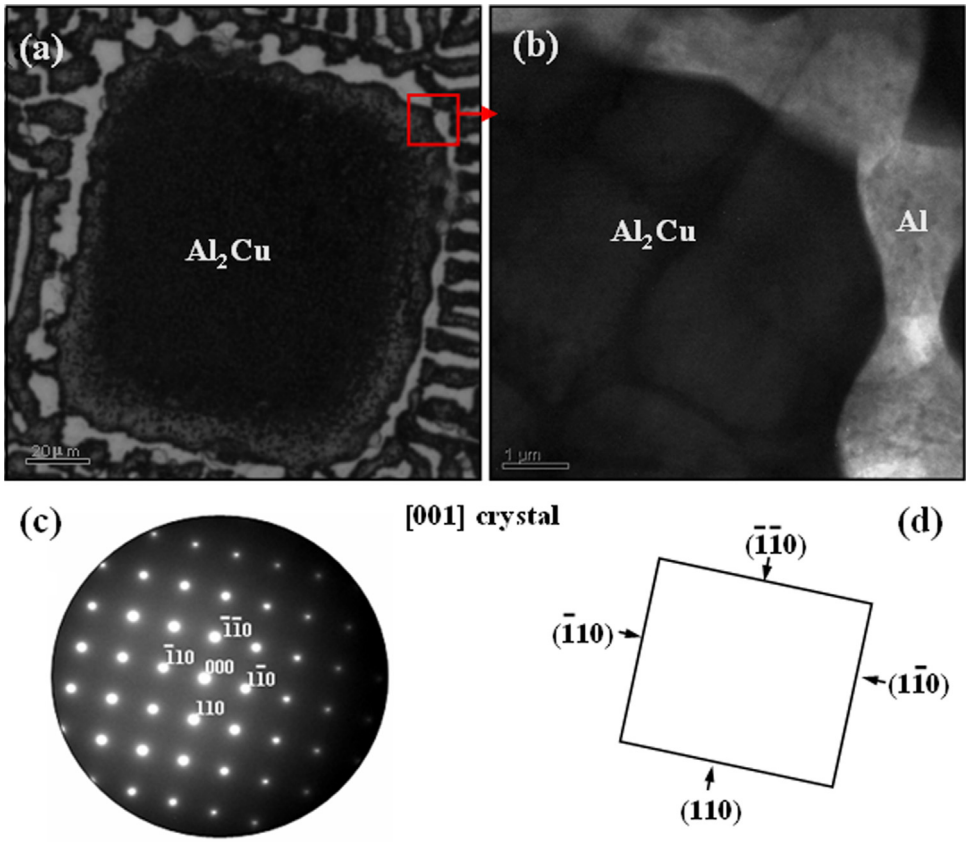

Fig. 7. (a) Transverse-section SEM image of rectangular pattern about the Al_2Cu phase in the 0.45 mm sample, (b) TEM image of the red region, (c) selected-area electron diffraction pattern (SAED) from the Al_2Cu phase in (b), [001] zone axis and (d) {110} facets image. (For interpretation of the references to color in this figure legend, the reader is referred to the web version of this article.)

Al_2Cu phase. The diffraction patterns in Fig. 8c show the same characteristic as that in Fig. 7c. The relationship between {110} facets and the surface of L-shaped morphology can be identified in Fig. 8d.

4. Discussion

Provided with a constant solidification rate of 10 μm/s, the growth morphology of the primary intermetallic Al_2Cu phase can vary remarkably for the directionally solidified samples in different sizes. To find the cause of this phenomenon, we first use the oriented attachment (OA) mechanism [22] to describe the microstructure evolution of the primary phase in the directionally solidified Al–40% Cu alloy. The oriented attachment mechanism is important to modify the morphology, and affects the final morphology and direction of crystalline growth according to the distribution of surface energy.

Fig. 9 shows the morphology evolution of the primary intermetallic Al_2Cu phase. To start with, tiny crystalline nucleus form in liquid and are followed by the aggregation of the nuclei. Larger particles will survive and engulf the smaller ones. The Al_2Cu phase will keep its regular crystal structure during growth at a small undercooling, since it belongs to a tetragonal structure.

As growing to bigger sizes, some small single Al_2Cu crystals will self-assemble into an L-shaped morphology through an oriented attachment mechanism shown in Fig. 9. The adjacent crystals become accumulated by sharing a common crystallographic orientation and these crystals dock at a planar interface. When the sample size decreases from 4 mm to 0.45 mm, the microstructures formed under diffusive growth conditions. The (310) direction would become predominant. The phase will grow more rapidly along the normal direction of the (310) crystal plane than in the (110) direction. Finally only the (110) crystal plane remains. It is noted that the (110) plane was also verified as the oriented attachment plane for being the largest faceted plane in the solidified microstructures [23]. The driving force for the above-mentioned spontaneous oriented attachment of the neighboring crystals is elimination of the pairing of the energy surfaces, leading to a substantial free energy reduction on the surface and interface instability. As a result, the Al_2Cu crystals fold to form an L-shaped morphology and further transform to an E-shaped morphology as indicated in Fig. 9. If the E-shaped microstructures collapse and merge into a unity, a rectangular pattern of the Al_2Cu phase can be observed. This result corresponds with the TEM results of the Al_2Cu phase surfaces shown in Figs. 7 and 8.

If there is any remaining liquid in the center of the rectangular pattern of the Al_2Cu phase, it will transform to eutectic microstructures as shown in Fig. 3c. Interestingly, some faceted microstructures, e.g., Si and intermetallic Mg_2Si, also possess smooth holes or cavities filled by the eutectics. These smooth holes may be caused by re-melting of the solidification front or dissolving of the local crystal surface in the presence of impurities [24]. This is different from the growth mechanism shown in Fig. 9. Unlike the two-dimensional nucleation and screw dislocation growth mechanisms that are responsible for the formation of faceted phase grown from melt, the oriented attachment mechanism can explain the microstructure evolution of the primary phase, correlating well with the experimental results shown in Figs. 3 and 4. Thus, by controlling the directional heat flux in the sample, the primary Al_2Cu phase can continuously grow along the preferred orientation. This may provide a microstructure maneuvering method for directional solidification of this alloy.

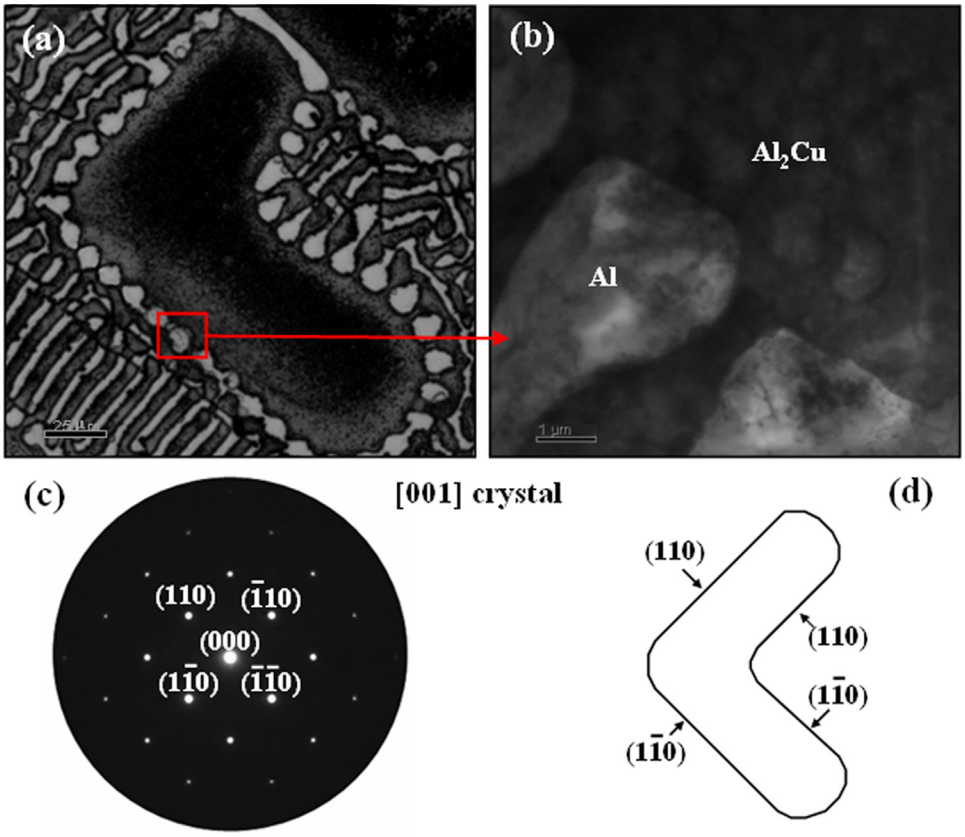

Fig. 8. (a) L-shaped morphology of Al_2Cu phase in the 4 mm sample by SEM, (b) TEM image of the red region, (c) selected-area electron diffraction pattern (SAED) from the Al_2Cu phase in (b), [001] zone axis, and (d) {110} facets image. (For interpretation of the references to color in this figure legend, the reader is referred to the web version of this article.)

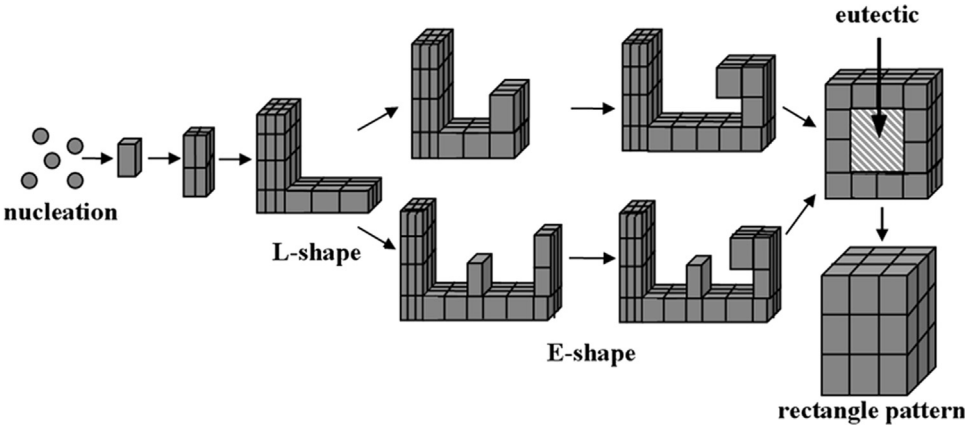

Fig. 9. The diagram of the morphology evolution of Al_2Cu phase in the transverse section.

5. Conclusions

Directionally solidified Al–40% Cu alloy samples in different sizes (4 mm, 1.8 mm, and 0.45 mm) have been prepared at a growth rate of 10 μm/s. The microstructure and crystal orientation of intermetallic dendrites Al_2Cu were investigated by changing the sample size. The main findings are summarized below.

(1) Different growth patterns of primary intermetallic Al_2Cu phase on 2D and 3D, including L-shaped, E-shaped, and rectangular morphologies were observed. The bounded surfaces of L-shaped and regular rectangular shape about Al_2Cu phase are {110} facets determined by TEM. The primary phase grew in a faceted way, which can be explained with an oriented attachment mechanism.
(2) By employing XRD measurement, a texture orientation at the (310) plane of the Al_2Cu phase was obtained in the 0.45 mm sample, different from the (110) plane of the Al_2Cu phase solidified in the 4 mm and 1.8 mm samples.
(3) The sample size can affect the microstructure and orientation of the Al_2Cu phase. A directional solidified Al–40% Cu alloy sample in a much smaller size can achieve a well-aligned morphology with a specific growth texture.

Acknowledgments

This work was financially supported by the National Natural Science Foundation of China through Grant nos. 50971101 and 51074127 and Project no. SKLSP201010.

References

[1] A. Okada, K. Toko, K.O. Hara, N. Usami, T. Suemasu, J. Cryst. Growth 356 (2012) 65–69.
[2] X.Q. Meng, C.T. Yang, J.C. Yang, J. Cryst. Growth 386 (2014) 57–61.
[3] K. Li, D. Rémiens, J. Costecalde, N. Sama, G. Du, T. Li, X.L. Dong, G.S. Wang, J. Cryst. Growth 377 (2013) 143–146.
[4] M.A. Salgado-Ordorica, A.B. Phillion, M. Rappaz, Metall. Mater. Trans. A 44 (2013) 2699–2706.
[5] J. Warren, Nat. Mater. 5 (2006) 595–596.
[6] T. Haxhimali, A. Karma, F. Geonales, M. Rappaz, Nat. Mater. 5 (2006) 660–664.
[7] X.B. Zhao, L. Liu, S.F. Gao, B.M. Ge, J. Zhang, Y. Li, H.Z. Fu, Cryst. Res. Technol. 46 (2011) 1291–1295.
[8] M. Amoorezaei, S. Gurevich, N. Provatas, Acta Mater. 60 (2012) 657–663.
[9] C.J. Li, H. Yang, Z.M. Ren, W.L. Ren, Y.Q. Wu, J. Alloys Compd. 505 (2010) 108–112.
[10] R. Hamar, C. Lemaignan, J. Cryst. Growth 53 (1981) 586–590.
[11] F. Yilmaz, R. Elliott, J. Cryst. Growth 66 (1984) 465–468.
[12] R. Trivedi, S. Liu, P. Mazumder, E. Simsek, Sci. Technol. Adv. Mater. 2 (2001) 309–320.
[13] K. Gao, S.M. Li, H.Z. Fu, Adv. Mater. Lett. 2 (2011) 368–372.
[14] R.S. Sidhu, N. Chawla, Mater. Charact. 52 (2004) 225–230.
[15] S.I. Lieberman, A.M. Gokhalea, S. Tamirisakandala, Scr. Mater. 55 (2006) 63–68.
[16] F.P. Dai, B.B. Wei, Sci. China Ser. E 52 (2009) 848–855.
[17] W.W. Zhu, Z.M. Ren, W.L. Ren, Y.B. Zhong, K. Deng, Mater. Sci. Eng. A 441 (2006) 181–186.
[18] J. Król, Mater. Des. 18 (1997) 345–347.
[19] R. Trivedi, H. Miyahara, P. Mazumder, E. Simsek, S.N. Tewari, J. Cryst. Growth 222 (2001) 365–379.
[20] Z.R. Feng, J. Shen, W. Wang, L.S. Wang, J.F. Zhang, Y.J. Du, H.Z. Fu, Metall. Mater. Trans. A 44 (2013) 640–649.
[21] D.M. Stefanescu, Science and Engineering of Casting Solidification2nd ed., Springer, Berlin, 2009.
[22] Q. Zhang, S.J. Liu, S.H. Yu, J. Mater. Chem. 19 (2009) 191–207.
[23] R. Bonnet, M. Loubradou, Phys. Status Solidi A 194 (2002) 173–191.
[24] H. Singh, A.M. Gokhale, Y. Mao, A. Tewari, A.K. Sachdev, Metall. Mater. Trans. B 40 (2009) 859–870.